PHYSICAL REVIEW D **78,** 034036 (2008)

Electric-magnetic asymmetry of the A^2 condensate and the phases of Yang-Mills theory

M. N. Chernodub[1] and E.-M. Ilgenfritz[2]

[1]*ITEP, Bolshaya Cheremushkinskaya 25, Moscow, 117259, Russia*

[2]*Institut für Physik, Humboldt-Universität zu Berlin, Newton-Strasse 15, 12489 Berlin, Germany*

(Received 29 May 2008; published 29 August 2008)

We study the finite-temperature behavior of the A^2 condensate in the Landau gauge of $SU(2)$ Yang-Mills theory on the lattice in a wide range of temperatures. The asymmetry between the electric (temporal) and magnetic (spatial) components of this unconventional dimension-2 condensate is a convenient ultraviolet-finite quantity which possesses, as we demonstrate, unexpected properties. The low-temperature behavior of the condensate asymmetry suggests that the mass of the lowest thermal excitation in the condensate is unexpectedly low, about 200 MeV, which is much smaller than the glueball mass. The asymmetry is peaking at the phase transition, becoming a monotonically decreasing function in the deconfinement phase. A symmetric point is reached in the deconfinement phase at a temperature approximately equal to twice the critical temperature. The behavior of the electric-magnetic asymmetry of the condensate separates the phase diagram of Yang-Mills theory into three regions. We suggest that these regions are associated with the condensed, liquid, and gaseous states of the confining gluonic objects, the Abelian monopoles.

DOI: 10.1103/PhysRevD.78.034036 PACS numbers: 12.38.Aw, 11.15.Ha, 25.75.Nq

I. INTRODUCTION

In a specific theoretical frame, nonperturbative features of QCD are reflected by the existence of various nonvanishing local condensates. The most famous vacuum condensates are the dimension-4 gluon condensate $\langle \alpha_s (G^a_{\mu\nu})^2 \rangle$ and the dimension-3 quark condensate $\langle \bar{\psi}\psi \rangle$. The former characterizes the nonperturbative dynamics of strongly interacting gluon fields while the latter—in the formal limit of vanishing quark masses—is an order parameter corresponding to the spontaneous breaking of chiral symmetry. The local condensates enter the QCD sum rules as nonperturbative power corrections having great significance for QCD phenomenology [1].

The dimension-2 condensates represent somewhat unconventional vacuum condensates. Indeed, it is impossible to construct dimension-2 operators in QCD in a gauge-invariant and local manner, simultaneously. One has to abandon either the condition of locality or the requirement of gauge invariance. Nonlocal but gauge-invariant operators are useless from the point of view of the operator product expansion: one cannot relate a nonlocal operator to a Wilson coefficient corresponding to a power correction using the dimensionality counting rule. On the other hand, the local but gauge-dependent operators seem to be useless because, as one might naively think, these operators cannot contribute to physical observables. However, this conclusion does not seem to be compelling, as it was pointed out in Refs. [2,3].

The simplest dimension-2 operator in $SU(N_c)$ gauge theory is[1]

$$A^2(x) = \sum_{a=1}^{N_c^2-1} \sum_{\mu=1}^{4} A^a_\mu(x) A^a_\mu(x). \tag{1}$$

This operator is not gauge invariant. Therefore, its expectation value can be understood in a twofold way: one can either average the operator over all possible gauge transformations or evaluate the operator at a particular point of a gauge orbit. The former choice leads to the unwanted nonlocality while the latter is a suitable option in particular gauges. The Landau gauge is defined as the result of minimization of the bulk averaged A^2 operator with respect to gauge transformations. Thus, the extremum of the dimension-2 operator gets a special meaning since $A^2(x)$ is a local operator in the Landau gauge.

The dimension-2 condensate enters the ultraviolet asymptotics of the gluon propagator in the Landau gauge as a nonperturbative powerlike $1/p^2$ correction. Moreover, this condensate emerges also in QCD in the quark propagator and in various vertices in the Landau gauge [4]. It is worthwhile to remember that for a long time it was as-

[1]In this paper we are working in $D = 4$-dimensional Euclidean space-time suitable for numerical lattice simulations of the $(3 + 1)$-dimensional $SU(2)$ gauge theory. The phase transition in this theory is of second order, while in the more interesting case of SU(3) gauge theory, the phase transition is of (weak) first order.

sumed that, due to asymptotic freedom, the whole physics at short distances must be described by exclusively perturbative physics. The appearance of the dimension-2 operator in the ultraviolet regime is a signature of mixing of nonperturbative and perturbative features of QCD: nonperturbative effects are emerging at very short distances.

Besides the purely theoretical issue of mixing ultraviolet and infrared physics, the appearance of the dimension-2 condensate plays a distinguished role in QCD phenomenology because it is associated with nonstandard power corrections [2,3,5]. This motivated the wide interest in the subject, such that the A^2 condensate was intensively studied both numerically and analytically. Numerical simulations of lattice $SU(3)$ Yang-Mills theory at zero temperature indicate that the A^2 condensate is, in fact, a large quantity [6],

$$\langle g^2 A^2 \rangle = [1.64(15)\ \mathrm{GeV}]^2. \tag{2}$$

The energy scale of the dimension-2 condensate (2) is of the order of the glueball mass [7,8],

$$m_{O^{++}} = 3.52(12)\sqrt{\sigma(T=0)} = 1.55(5)\ \mathrm{GeV}, \tag{3}$$

if one takes the phenomenologically accepted value $\sigma(T = 0) = [440\ \mathrm{MeV}]^2$ for the string tension at zero temperature. The coincidence does not look accidental. Of course, the appearance of the dimension-2 condensate and the mass gap generation in the non-Abelian gauge theory are both of nonperturbative nature.

Another nonperturbative phenomenon in non-Abelian gauge theory is the confinement of color, which is often linked with the mass gap generation, but the relevant scale is $\Lambda_{\mathrm{QCD}} \sim 200$ MeV. A relation between the dimension-2 condensate and color confinement may also exist, although the very reason is not clear at present. A good playground to study the interrelations between the different mentioned nonperturbative features would be a suitably chosen effective (toy) model. The confinement of electric charges and the mass gap generation is understood, for example, in the framework of an Abelian gauge model with a compact gauge field, which can be considered as a certain limit of the $SO(3)$ Yang-Mills-Higgs model (often called the Georgi-Glashow model). The compactness of the gauge field is related to the presence of nonperturbative objects, magnetic monopoles, the dynamics of which leads both to confinement and to mass gap generation [9].

The four-dimensional version of the compact Abelian gauge model [sometimes called "compact electrodynamics" or $cU(1)$ gauge theory] contains two phases—the confinement phase and the deconfinement phase—separated by a phase transition. At zero temperature this model is especially interesting since the phases of the model are characterized by a single parameter, the gauge coupling g. The confinement phase is located at strong coupling, $g > g_c \sim 1$, while the deconfinement regime is associated with weak coupling. The confinement phenomenon comes along with the mass gap generation, while in the deconfinement phase the mass gap shrinks to zero. Both mass gap and charge confinement have the same, well-understood [10] roots in the condensation of the Abelian monopoles (for a review see Refs. [11,12]). The natural question to ask is "does an A^2 condensate appear in the compact Abelian model?" If the answer is positive, what can we say about a possible relation between confinement/mass gap generation and the emergence of the A^2 condensate? These questions were addressed in Ref. [2], where it was found that the nonperturbative part of the A^2 condensate in the Landau gauge is a very good order parameter for the confinement-deconfinement phase transition: this dimension-2 condensate is nonvanishing in the confinement phase and vanishes in the deconfinement phase. In the compact Abelian model the link between all three phenomena—confinement, mass gap generation, and the emergence of the dimension-2 condensate—is obvious: the primary reason for all these phenomena is monopole condensation.

Coming back to the Yang-Mills theory, one finds an essential difference between this theory and the just discussed Abelian model: the transition in the pure Yang-Mills theory is driven by thermal fluctuations and, therefore, it happens at finite temperature. On the contrary, in the mentioned simulations of the compact Abelian gauge theory the transition is purely quantum, and thermal fluctuations are not involved. In finite-temperature Yang-Mills theory (and in QCD as well), instead of having one dimension-2 condensate (1) one needs to define two types, corresponding to timelike ("electric") and to spacelike ("magnetic") gauge bosons, separately. In the Euclidean imaginary-time formalism at $T \neq 0$, one defines the electric and magnetic contributions, respectively:

$$A_E^2 = \frac{1}{N_c}\,\mathrm{Tr} A_4(x) A_4(x), \qquad A_M^2 = \frac{1}{N_c}\,\mathrm{Tr}\sum_{i=1}^{3} A_i(x) A_i(x), \tag{4}$$

such that the full dimension-2 condensate at nonzero temperature is the sum of both,

$$\langle g^2 A^2 \rangle = \langle g^2 A_E^2 \rangle + \langle g^2 A_M^2 \rangle. \tag{5}$$

In Eq. (4) we have not yet divided the magnetic contribution by the number of spatial dimensions. This would make $\langle g^2 A_E^2 \rangle$ and $\langle g^2 A_M^2 \rangle$ the dimension-2 condensate per one Lorentz component (or per three Lorentz components) of the electric (magnetic) gluons in the Landau gauge. We refine the conclusion of Ref. [13] that the A^2 condensate observed at zero temperature is consistent with a vanishing condensate in the deconfinement phase. In fact, the condensate at finite temperature is characterized by the electric and magnetic components which, as we show, are quite nontrivial. To our knowledge, the eventual difference between the two simplest dimension-2 condensates has not been considered so far. In this paper we fill this gap.

Before proceeding further, one should comment about the ultraviolet divergences of the dimension-2 condensate. In compact electrodynamics [2] at vanishing temperature, the condensate contains perturbative and nonperturbative parts, respectively,

$$\langle g^2A^2\rangle = \langle g^2A^2\rangle_{\rm pert} + \langle g^2A^2\rangle_{\rm NP}. \tag{6}$$

The perturbative part is quadratically divergent whereas the nonperturbative part is finite. The first one can be calculated trivially in noncompact QED, the free theory of photons. It is the nonperturbative part which serves as the order parameter of the nonthermal phase transition in compact electrodynamics.

In QCD the situation is similar but not so simple [6,14,15]. A linear decomposition (6) works as well up to renormalization-related logarithmic corrections. Then in Eq. (6) $\langle g^2A^2\rangle_{\rm pert} \propto \Lambda^2_{\rm UV}$ and $\langle g^2A^2\rangle_{\rm NP} \propto \Lambda^2_{\rm QCD}$, where $\Lambda_{\rm QCD}$ defines a typical QCD energy scale—supplemented with a large prefactor according to Eq. (2)—while $\Lambda_{\rm UV} \propto 1/a$ is an ultraviolet cutoff, which in the case of lattice calculations is inversely proportional to the lattice spacing a. The calculation of the nonperturbative part of the condensate requires a renormalization which was implemented, for example, in Ref. [6].

At finite temperature the decomposition (6) should hold as well. It is well known that the finite-temperature corrections to physical observables do not contain ultraviolet divergences. However, the temperature corrections can be both of perturbative and nonperturbative nature such that they can affect both the perturbative and nonperturbative parts of the decomposition (6).

In our numerical analysis we do not discriminate between perturbative and nonperturbative parts. Of course, we distinguish between corrections received by the spatial (magnetic) and temporal (electric) gluons. On general grounds, we write the decomposition per Lorentz component in the form

$$\langle g^2A^2\rangle_E = \tfrac{1}{4}\langle g^2A^2\rangle_0 + \langle g^2A_E^2\rangle_T, \tag{7}$$

$$\langle g^2A^2\rangle_M = \tfrac{3}{4}\langle g^2A^2\rangle_0 + \langle g^2A_M^2\rangle_T, \tag{8}$$

where $\langle g^2A^2\rangle_0$ is the dimension-2 condensate at zero temperature while $\langle g^2A^2_{E(M)}\rangle^T$ is the finite-temperature correction to the electric (magnetic) dimension-2 condensate. These thermal corrections are ultraviolet finite at finite T and are vanishing at $T = 0$. It is the zero-temperature condensate $\langle g^2A^2\rangle_0$ that contains a piece which is quadratically divergent in the ultraviolet. In the limit of zero temperature, magnetic and electric components are equal and expressed naturally via the zero-temperature condensate. In this limit the sum rule (5) is also naturally restored.

We suggest concentrating on the thermal corrections to the condensates, $\langle g^2A_E^2\rangle_T$ and $\langle g^2A_M^2\rangle_T$, as probes of the thermal activity of the electric and magnetic components, respectively, of the gluonic medium. In this paper we compute the electric-magnetic asymmetry of the dimension-2 condensate,

$$\Delta_{A^2}(T) = \langle g^2A_E^2\rangle - \frac{1}{3}\langle g^2A_M^2\rangle \equiv \langle g^2A_E^2\rangle_T - \frac{1}{3}\langle g^2A_M^2\rangle_T$$
$$= \langle g^2A_4^2\rangle_T - \frac{1}{3}\sum_{i=1}^{3}\langle g^2A_i^2\rangle_T. \tag{9}$$

The asymmetry (9) plays a special role since the quadratically divergent zero-temperature components of both electric and magnetic condensates cancel out. Thus the asymmetry (9) is a finite-valued quantity in the ultraviolet regime.

We have calculated the asymmetry (9) using numerical simulations of Yang-Mills lattice gauge theory in the Landau gauge. Obviously, at zero temperature (symmetric lattice) all Lorentz components of the gauge field A_μ contribute equally to the A^2 condensate because of the approximate $O(4)$ rotational symmetry [actually $H(4)$ hypercubic symmetry] satisfied by the Euclidean lattice. At finite temperature this rotational symmetry is broken down to (approximate) $O(3)$ spatial symmetry. Space and time coordinates are no longer equivalent since, in the imaginary-time formalism used to study the field in a thermodynamic equilibrium state, a finite temperature T is implemented via compactification of the (imaginary) time direction to a circle of length $L_t = 1/T$, while the other (spatial) directions L_s are still infinite, or at least $L_s \gg L_t$. Thus, the fluctuations of the temporal (electric) A_4 and spatial (magnetic) A_i ($i = 1, 2, 3$) components of the gluon fields must be different, in general.

The structure of this article is as follows. In Sec. II we describe the theoretical expectations. In Sec. III we report our lattice simulations for $SU(2)$ pure gauge theory. Section IV contains a discussion relating our findings to monopoles and confinement. We draw conclusions and define further routes in Sec. V.

II. THEORETICAL EXPECTATIONS

The low- and high-temperature asymptotics of the electric-magnetic asymmetry of the dimension-2 condensate Δ_{A^2} can be guessed from general arguments:

$$\Delta_{A^2}(T) \propto \begin{cases} e^{-(m_{\rm gl}/T)} & T \ll T_c, \\ T^2 & T \gg T_c. \end{cases} \tag{10}$$

It is tempting to equate the mass parameter $m_{\rm gl}$ with the mass of the lowest glueball:

$$m_{\rm gl} = m_{O^{++}} \quad \text{(naive expectation)}. \tag{11}$$

In Eq. (10) a polynomial prefactor at low temperatures and possible logarithmic corrections at high temperatures are omitted. The high-temperature asymptotics in Eq. (10) is determined for dimensional arguments. In the results of lattice simulations, we will show that the dimensional argument is correct, as expected.

Common wisdom says that the low-temperature asymptotics of any thermodynamic system is determined by properties of the lowest excitation. The lowest excitation in the $SU(N_c)$ gauge theory is a glueball, which has a nonzero mass due to the phenomenon of the mass gap generation. According to Ref. [7], in the $SU(3)$ gauge theory $m_{O^{++}} = 3.52(12)\sqrt{\sigma(T=0)}$. According to the Bielefeld group, Refs. [16,17], the finite-temperature phase transition in pure $SU(3)$ gluodynamics happens at $T_c = 0.629(3)\sqrt{\sigma(T=0)}$ such that $m_{O^{++}} \approx 5.6 T_c$. Given that $m_{O^{++}} \gg T_c$ the low-temperature asymptotics should hold true not only at $T \ll T_c$, but also at temperatures close to the phase transition temperature. As we will see below, in Yang-Mills theory the exponential form of the low-temperature asymptotics is correct, while, unexpectedly, the "natural" identification of mass scale (11) turns out to be wrong. Moreover, the low-temperature asymptotics (10) of the asymmetry turns out to be also incorrect in certain simple models, indicating that the exponential low-temperature asymptotics (10) is not valid in a general case.

We begin the discussion of the asymmetry in the simplest case of free photodynamics, and then for the Abelian Higgs model. After that, we turn to the case of Yang-Mills theory.

A. Example of photodynamics

Photodynamics is the theory of the free Abelian gauge field. Since the theory does not contain any dimensional scale and is not able to generate a scale by itself like QCD, the electric-magnetic asymmetry of the A^2 condensate—which is the dimension-2 quantity $\Delta_{A^2}(T)$—must be proportional to T^2 for dimensional reasons.

Since the Lagrangian of photodynamics is quadratic,

$$\mathcal{L}_{\text{phot}} = \tfrac{1}{4} F_{\mu\nu}^2, \qquad F_{\mu\nu} = \partial_\mu A_\nu - \partial_\nu A_\mu, \tag{12}$$

it is easy to calculate the photon correlation function (propagator) in momentum space,

$$\langle \tilde{A}_\mu(p) \tilde{A}_\nu(-p) \rangle = D_{\mu\nu}(p), \tag{13}$$

where $p = (\mathbf{p}, p_4)$ is the 4-momentum, while the relation between the photon fields in coordinate and momentum spaces is given by Fourier transformation. At zero temperature the relation is

$$A_\mu(x) = \int \frac{\mathrm{d}^4 p}{(2\pi)^4} e^{i(p,x)} \tilde{A}_\mu(p), \qquad T = 0, \tag{14}$$

while at finite temperature it is given by the formula

$$A_\mu(x) = \int \frac{\mathrm{d}^3 p}{(2\pi)^3} T \sum_n e^{i(\mathbf{p},\vec{x}) + i\omega_n x_4} \tilde{A}_\mu(\mathbf{p}, \omega_n), \qquad T \neq 0, \tag{15}$$

where

$$\omega_n = 2\pi n T \tag{16}$$

are the Matsubara frequencies.

Because of the absence of interactions the form of the (zero-temperature) photon propagator,

$$D_{\mu\nu}(p) = D(p^2)\left(\delta_{\mu\nu} - \frac{p_\mu p_\nu}{p^2}\right), \tag{17}$$

is also valid at finite temperature. The propagator (17) is parametrized by a single propagator function (here $p^2 = \mathbf{p}^2 + p_4^2$):

$$D(p^2) \equiv D^{\text{photo}}(p^2) = \frac{1}{p^2}. \tag{18}$$

The asymmetry of the dimension-2 condensate in photodynamics is calculated in Appendix A:

$$\Delta_{A^2}^{\text{free}}(T) = \frac{1}{3\pi^2} \int_0^\infty \mathrm{d}p\, p^2 f_T(p) \left\{ \frac{1}{2p} - \frac{1}{T}[1 + f_T(p)] \right\} = -\frac{T^2}{12}. \tag{19}$$

As the definition of the asymmetry, we took Eq. (9) with a one-component gauge field, $N_g = 1$. We have also omitted the overall coefficient, electric charge squared, $g^2 = e^2$, in the definition (9) in order to simplify the expressions below. This coefficient can easily be restored: it should enter all the analytic results of this section for the asymmetry as just the proportionality coefficient. The proportionality of the asymmetry to the squared temperature in Eq. (19) is quite obvious due to dimensionality reasons. The fact that the asymmetry (19) is negative tells us that in the absence of the interactions the fluctuations of the magnetic (spatial) photons are dominating the fluctuations of the electric (temporal) photons.

B. Example of Abelian Higgs model

Now we turn to a more complicated case, adding a charged scalar field to the photodynamics. This system is described by the Abelian Higgs model with the Lagrangian

$$\mathcal{L}_{\text{AHM}} = \tfrac{1}{4} F_{\mu\nu}^2 + |(\partial_\mu + ieA_\mu)\phi|^2 + \lambda(|\phi|^2 - \eta^2)^2, \tag{20}$$

and controlled by the gauge coupling e and the quartic coupling λ. The overall dimensional scale is fixed by the position η of the minimum of the potential for the Higgs field ϕ.

In the Higgs phase the photon has a mass $m = e\eta$ due to spontaneous symmetry breaking caused by the condensation of the scalar Higgs field. At zero temperature the photon propagator is described by Eq. (17) with the single propagator function

$$D(p) = D^{\text{AHM}}(p) = \frac{1}{p^2 + m^2}. \tag{21}$$

In the case of the London limit, $\lambda \to \infty$, with the Higgs field being infinitely massive, the latter is not thermally excited if the system is subject to finite temperatures. As a result, the Higgs loops do not contribute to the photon polarization tensor. The difference between spatially longitudinal and spatially transverse photons is absent in this case, as they share the same propagator function (21). Then, the Lorentz structure at finite temperature of the gauge propagator stays the same as in Eq. (17).

The asymmetry for the London limit is calculated in Appendix B:

$$\Delta^{\mathrm{AHM}}_{A^2}(T,m) = \frac{4}{3m^2}[\varepsilon(T,m) - \varepsilon(T,m=0)] - \frac{1}{3}\Sigma(T,m), \tag{22}$$

where

$$\varepsilon(T,m) = \int \frac{\mathrm{d}^3p}{(2\pi)^3}\sqrt{\mathbf{p}^2+m^2}\, f_T(\sqrt{\mathbf{p}^2+m^2}) \tag{23}$$

and

$$\Sigma(T,m) = \int \frac{\mathrm{d}^3p}{(2\pi)^3}\frac{1}{\sqrt{\mathbf{p}^2+m^2}} f_T(\sqrt{\mathbf{p}^2+m^2}). \tag{24}$$

In Fig. 1 we show the asymmetry (22) divided by the temperature squared T^2 as a function of the temperature T expressed in units of the gauge boson mass m.

In the massless limit, $m \to 0$, the asymmetry (22) can be calculated exactly:

$$\lim_{m\to 0}\Delta^{\mathrm{AHM}}_{A^2}(T,m) = -\frac{T^2}{12}. \tag{25}$$

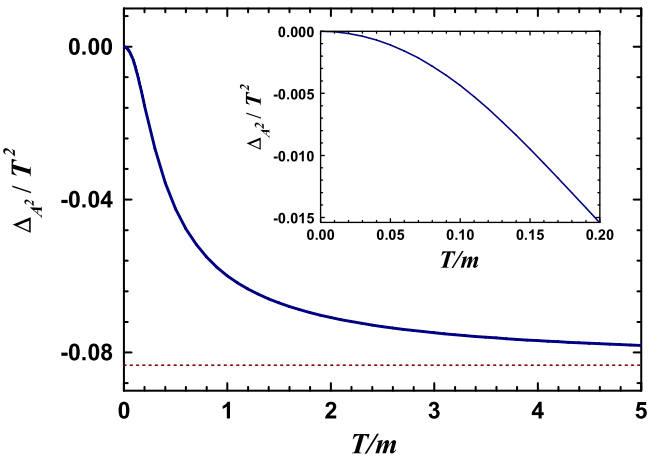

FIG. 1 (color online). The normalized electric-magnetic asymmetry of the A^2 condensate, $\Delta_{A^2}(T,m)/T^2$, as a function of the normalized temperature, T/m, in the Abelian Higgs model. The horizontal dashed line in the plot shows the high-temperature limit (27), for $T \gg m$, which recovers the case of photodynamics. The inset illustrates the low-temperature behavior of the condensate asymmetry (28).

The comparison of Eq. (25) with Eq. (19) shows that the A^2 asymmetry is an analytic function of the photon mass at $m = 0$:

$$\lim_{m\to 0}\Delta^{\mathrm{AHM}}_{A^2}(T,m) = \Delta^{\mathrm{AHM}}_{A^2}(T,0) \equiv \Delta^{\mathrm{photo}}_{A^2}(T). \tag{26}$$

This result is, in fact, not guaranteed from the beginning—as we describe in the appendixes—since the exactly massless case involves the calculation of a residue at the double pole while the massive theory always has two isolated single poles in the asymmetry.

Equation (25) corresponds, in fact, to the leading term in the asymmetry in the high-temperature limit, $T \gg m$. Supplementing this result with the low-temperature expansion, we get the leading terms in high- and low-temperature limits, respectively:

$$\Delta_{A^2}(T,m) = -\frac{T^2}{12} + \ldots \qquad (T \gg m), \tag{27}$$

$$\Delta_{A^2}(T,m) = -\frac{2\pi^2}{45}\frac{T^4}{m^2} + \ldots \qquad (T \ll m), \tag{28}$$

where the ellipses denote subleading contributions.

As we have expected, the difference between the electric and magnetic components of the condensate in the Abelian Higgs model is vanishing in the zero-temperature limit according to Eq. (28). What is unexpected is that at low temperatures the asymmetry is suppressed polynomially (by the fourth power of the temperature, T^4) and not exponentially as one would have expected from general arguments presented in the beginning of this section. Indeed, the Abelian Higgs model is a theory with a finite mass gap, and therefore one could expect that thermodynamical contributions to any quantity would be suppressed exponentially in the low-temperature limit by a factor $\exp\{-m/T\}$. Our analytical calculation shows this is not the case.

Technically, the unusual polynomial behavior $\Delta_{A^2}(T,m) \propto T^4$ of the asymmetry at low temperatures is due to the massless, $m = 0$, term in Eq. (22). This term corresponds to a massless longitudinal degree of freedom, while all other terms are massive such that they are suppressed exponentially as $T \ll m$. The appearance of this term can be traced in the integrand (B2) of the integral representation of the asymmetry (A11), as this integrand contains a massless pole. The massless pole, in turn, appears due to the fact that the propagator of the gauge boson (17) contains a $1/p^2$ term which does not give any contribution in explicitly transverse gauge-invariant expressions, such as the correlator of two field strength tensors. However, the A^2 propagator *does* incorporate an infrared $1/p^2$ term, which gives rise to a polynomial behavior unless the propagator function $D(p)$ is vanishing in the infrared. Both in photodynamics and in the Abelian Higgs model the photon propagator is either divergent or finite in the infrared limit such that the zero-temperature limit of

the asymmetry is not exponentially suppressed, contrary to our naive expectation (10).

C. Distinguishing longitudinal and transverse photons

Contrary to the considered examples, at finite temperature the gluon propagator in the Landau gauge is, in general, parametrized by two propagator functions. These are the transverse (or magnetic) propagator D_T and the longitudinal (or electric) propagator D_L. In momentum space,

$$D^{ab}_{\mu\nu}(\mathbf{p}, p_4) = \delta^{ab}[P^T_{\mu\nu} D_T(\mathbf{p}, p_4) + P^L_{\mu\nu} D_L(\mathbf{p}, p_4)]. \quad (29)$$

Here $P^T_{\mu\nu}$ and $P^L_{\mu\nu}$ are, respectively, projectors onto spatially transverse and spatially longitudinal directions [18], with

$$P^T_{\mu\nu} = (1 - \delta_{\mu 4})(1 - \delta_{\nu 4})\left(1 - \frac{p_\mu p_\nu}{\mathbf{p}^2}\right), \quad (30)$$

satisfying the relation

$$P^T_{\mu\nu} + P^L_{\mu\nu} = P_{\mu\nu}, \qquad P_{\mu\nu} = \delta_{\mu\nu} - \frac{p_\mu p_\nu}{p^2}, \quad (31)$$

where $P_{\mu\nu}$ is the standard $O(4)$-symmetric projector corresponding to the zero-temperature case with $p^2 = \mathbf{p}^2 + p_4^2$.

At finite temperature the propagators D_T and D_L are, in general, different from each other. The difference between spatially longitudinal and spatially transverse functions arises due to interactions among the fields, while in the free gauge theory these functions are equal: $D_T^{\text{free}} = D_L^{\text{free}}$. The interactions which lead to the difference between the propagators D_T and D_L may be perturbative, as, for example, in quantum electrodynamics [18], or these interactions can be of purely nonperturbative origin, as, for example, in an Abelian gauge theory which contains only a compact gauge field [19]. The compact Abelian gauge theory possesses nonperturbative topological defects, monopoles, which drastically affect the propagator properties in the confining phase of the theory.

In $SU(2)$ Yang-Mills theory the propagators D_T and D_L were investigated using both numerical simulations on the lattice [20] and analytical calculations in the continuum [21–24]. In the limit of vanishingly low temperatures the thermodynamics of Yang-Mills theory imposes a certain constraint on the infrared critical exponents which characterize the infrared behavior of the correlators [25].

From Eq. (29) one can derive the electric-magnetic asymmetry of the A^2 condensate in terms of the two propagators:

$$\Delta_{A^2}(T) = \frac{N_c^2 - 1}{24\pi^3} T \int \mathrm{d}^3\mathbf{p} \sum_n \left[\frac{3\mathbf{p}^2 - \omega_n^2}{\mathbf{p}^2 + \omega_n^2} D_L(\mathbf{p}, \omega_n) - 2 D_T(\mathbf{p}, \omega_n) \right]. \quad (32)$$

This expression should be ultraviolet finite up to a logarithmic renormalization.

III. NUMERICAL RESULTS IN $SU(2)$ YANG-MILLS THEORY

In the following we report measurements of the electric-magnetic asymmetry of the A^2 condensate that were performed in $SU(2)$ gluodynamics simulations. The configurations have been created by means of a heatbath Monte Carlo code. The minimal Landau gauge has been enforced for every 30th configuration before measuring the A^2_μ. For the gauge fixing we have used the simulated annealing algorithm [26]. An interval of the gauge temperature ranging from $T_{\max} = 1.0$ to $T_{\min} = 1.0 \times 10^{-5}$ has been traversed within 3000 sweeps with linearly decreasing gauge temperature. This "gauge cooling" was followed by obligatory over-relaxation until the required transversality was reached. The stopping criterion was $\max_x \max_a |(\partial_\mu A^a_\mu)(x)| < 10^{-9}$.

We have evaluated the electric-magnetic asymmetry on lattices $16^3 \times 4$, $24^3 \times 6$, and $32^3 \times 8$. In the interval $\beta \in [2.20, 2.95]$ we have selected a grid containing 51, 36, and 24 β values, respectively. In this way, an interval of physical temperatures $T \in [0.4T_c, 6.1T_c]$ is covered. In the restricted range $T \in [0.4T_c, 2.5T_c]$, systems at nearly equal temperatures are realized by lattices with different lattice spacings. Close to the deconfining transition, the $3D$ volumes are equal to each other with an aspect ratio of $N_s{:}N_t = 4{:}1$. The simultaneous evaluation of the asymmetry provides us with a valuable assessment of potentially dangerous finite cutoff effects. This does not seem to be a problem at all. As we will see later, data from different lattice sizes are smooth and can be fitted simultaneously as functions of the physical temperature.

The number of configurations at each combination of lattice size and β value was adjusted in such a way as to give reasonable statistical error bars (typically, the errors are of the order of a few percent near the phase transition temperature). Close to the transition we needed about 1500 configurations per β value at the smallest lattice, and we found about 50 configurations per value of β sufficient at the largest lattice far from the transition.

All our production measurements have been done with one Gribov copy only. We stress that the simulated annealing algorithm already shifts the outcome of a single gauge fixing closer to the (unknown) absolute maximum of the gauge functional than several repetitions of pure overrelaxation could do. We have actually checked the Gribov copy dependence at our middle-sized lattice, $24^3 \times 6$, for a representative set of four temperatures corresponding to the confinement region ($\beta = 2.30$, $T \approx 0.65T_c$) and to the deconfinement region ($\beta = 2.7$, $T \approx 2.4T_c$), and for two temperatures close to the phase transition, on the confinement ($\beta = 2.40$, $T \approx 0.9T_c$) and the deconfinement ($\beta = 2.50$, $T \approx 1.25T_c$) sides. We took the

first ten Gribov copies, $N_G = 1 \ldots 10$, by repeating the simulated annealing gauge fixing. To form the ensemble collecting the best gauge copies for each Monte Carlo configuration after N_G repetitions of simulated annealing, we sampled the "currently best" copy among the preceding N_G gauge-fixing trials. We found that—within our statistical errors—the plateau value (for the ensembles with $N_G \to \infty$) of the electric-magnetic asymmetry is already reached in the ensemble of gauge-fixed copies corresponding to $N_G \simeq 4$ trials. In the deconfinement phase the copy dependence is negligible since the systematical uncertainty due to the Gribov copy dependence is much smaller than the statistical errors of our calculations. In the confinement region the uncertainty—calculated as the relative deviation of the measured value of the electric-magnetic asymmetry after N_G trials from the $N_G \to \infty$ plateau value—is about 2%, while in the close neighborhood of the phase transition, the systematic correction to the electric-magnetic asymmetry due to Gribov copy dependence may reach 10%. The asymmetry is slightly rising with the number of gauge copies being under inspection. However, all characteristic features of the asymmetry discussed in this article are unaffected by this Gribov copy dependence.

The vector potential is extracted from the links as

$$gA^a_\mu(x + \hat{\mu}/2) = \mathrm{Tr}[\tau_a(U_{x,\mu} - U^\dagger_{x,\mu})/(2ia)]. \qquad (33)$$

We express all dimensional quantities in units of the critical temperature. According to Ref. [27] the phase transition—which is of the second order in pure $SU(2)$ gauge theory—happens at the critical temperature

$$T_c = 0.694(18)\sqrt{\sigma(T=0)} = 305(8)\ \mathrm{MeV}. \qquad (34)$$

The electric-magnetic asymmetry of the A^2 condensate (9) is shown in Fig. 2. One can observe a very good scaling: the results obtained at various lattice sizes describe the same curve when plotted in physical units. This fact indicates that the lattice ultraviolet artifacts are negligible in our numerical setup.

Before going into detail, we notice immediately two distinct features of the temperature dependence of the A^2 condensate asymmetry:

(i) The maximum is taken at $T = T_{\max} \approx T_c$. We observe a sharp maximum of Δ_{A^2}, signaling that the asymmetry of the gluonic medium is peaked around the phase transition.

(ii) There is a symmetric point, $T = T_0 \approx 2T_c$, where the asymmetry vanishes. This point is realized in the deconfinement phase sufficiently far from the phase transition at a temperature approximately equal to twice the critical temperature.

The mentioned points divide the phase diagram into three separate regions:

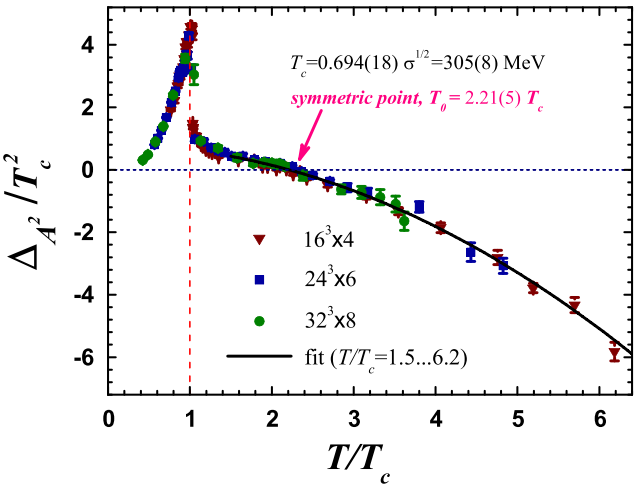

FIG. 2 (color online). The electric-magnetic asymmetry of the A^2 condensate (9) for $SU(2)$ gauge theory normalized by the critical temperature squared as a function of T/T_c. The high-temperature fit (39) with the best fit parameters (40) is shown by the solid line. The horizontal dashed line corresponds to $\Delta_{A^2} = 0$, while the vertical dashed line marks the critical temperature. The symmetric point is explicitly indicated.

(i) Region 1: The confinement phase, $T \lesssim T_c$. The asymmetry is a positive monotonically increasing function of temperature in the confinement region.

(ii) Region 2: The deconfinement phase at relatively low temperatures, $T_c \lesssim T < T_0$. Here the asymmetry is still positive valued and a monotonically decreasing function of temperature. The asymmetry vanishes at the temperature T_0, which we estimate below.

(iii) Region 3: The deconfinement phase at high temperatures, $T > T_0$. Here the asymmetry is negative valued and monotonically further decreasing as a function of temperature.

As we speculate below in Sec. IV, these regions are each characterized by a particular dynamics of the Abelian monopoles. These are singular configurations of the gluonic fields responsible for the confinement of color in the low-temperature phase. Region 1 corresponds to the phase where the monopoles are condensed. At higher temperatures, in region 2, the monopole condensate melts into a monopole liquid [28], whereas at even higher temperatures, in region 3, the liquid of the Abelian monopoles is suggested to evaporate into a gaseous state [28]. The transition between region 1 and region 2 is a true phase transition (turning the monopole condensate into a monopole liquid), whereas the transition between region 2 and region 3 (the evaporation of the monopole liquid) is suggested to be a broad crossover. The interaction with electric charges plays an important role in the dynamics of monopoles [29,30], such that we expect an effect of the changing monopole dynamics on the electric-magnetic asymmetry of the condensate.

The deconfining transition at $T = T_c$ has a noticeable effect on the asymmetry of the condensate since at this temperature the electric part of the condensate is maximally dominating over the magnetic one. This dominance is rapidly decaying just above T_c. We define the maximum as

$$\Delta_{A^2}^{\max} \equiv \max_T \Delta_{A^2}(T) = \Delta_{A^2}(T_{\max}). \tag{35}$$

We estimate the numerical value of the maximum as

$$\Delta_{A^2}^{\max} = [2.26(4)T_c]^2 \equiv [690(22)\ \text{MeV}]^2, \tag{36}$$

and the temperature

$$T_{\max} = 1.00(3)T_c \equiv 305(12)\ \text{MeV}. \tag{37}$$

The symmetric point is realized at a temperature at which the asymmetry of the condensate is vanishing. Our estimate of the symmetric point is

$$T_0 = 2.21(5)T_c = 675(23)\ \text{MeV}, \qquad \Delta_{A^2}(T_0) = 0. \tag{38}$$

The change of sign of Δ_{A^2} happens in the deconfinement phase at a temperature approximately twice the deconfinement temperature. In order to accurately estimate the position of the symmetric point (38), we performed a specific fit of the asymmetry throughout the deconfinement region.

The *high-temperature* fit is done with the help of the following fitting function:

$$\Delta_{A^2}^{\text{fit}} = \Delta_{A^2}^{(0)} - fT^2 \quad \text{(at high temperatures)} \tag{39}$$

where $\Delta_{A^2}^{(0)}$ and f are two fitting parameters. The form of the fitting function is inspired by the analytical examples provided by photodynamics (19) and by the Abelian Higgs model (27) in their high-temperature limits. Surprisingly, the fit works very well not only at very high temperatures, but also down to temperatures as low as $1.5T_c$. We obtain—with a $\chi^2_{\text{d.o.f.}} \approx 2$—the following best fit parameters:

$$\Delta_{A^2}^{(0)} = [0.894(14)T_c]^2 = [274(8)\ \text{MeV}]^2, \qquad f = 0.164(4). \tag{40}$$

The fit is shown in Fig. 2 by the solid line. According to the high-temperature limits in photodynamics (19) and in the Abelian Higgs model (27), one could have expected that each color component of the gluon would give the same contribution $g^2/12$ to the coefficient f in Eq. (40). For $N_g = N_c^2 - 1 = 3$ free gluons, this coefficient should be equal to $f = g^2/4$, indicating that $g \lesssim 1$. This result is expected since in the considered temperature regime the theory is still in a strongly nonperturbative regime. One should note that the quadratic fit (39) may mimic some other, nontrivial T dependence of the asymmetry, the exact form of which is difficult to figure out at our accuracy. The fit is convenient for the estimation of the symmetric point (38) which follows from Eqs. (39) and (40).

In order to emphasize the approach of the electric-magnetic asymmetry of the condensate to the asymptotic behavior at high temperatures, we present in Fig. 3 the asymmetry normalized by the temperature squared.

The *low-temperature* limit is especially interesting in view of the existence of two different options: although Yang-Mills theory possesses the mass gap, the asymmetry would not necessarily be exponentially suppressed, as suggested in Eq. (10). Indeed, the asymmetry could behave polynomially, according to our calculation (28) in the broken phase of the Abelian Higgs model. In order to figure out the behavior of the asymmetry, we have made an interpolating fit, which includes both options:

$$\Delta_{A^2}^{\text{fit}} = C_\Delta T_c^2 \left(\frac{T}{T_c}\right)^\nu \exp\{-m/T\} \quad \text{(at low temperatures)}. \tag{41}$$

The polynomial behavior would be realized if $m = 0$, while the exponential suppression is in effect with $m \neq 0$.

We show the low-temperature asymmetry in Figs. 4(a) and 4(b). In order to visualize the exponential behavior in Fig. 4(a) we took the logarithm of the asymmetry normalized by the dimensional factor T_c^2 and then multiplied the logarithm by $-T/T_c$. If the behavior of the asymmetry is proportional to the Boltzmann-like exponential function (without the polynomial prefactor), then the data must be linear in the low-temperature region. This is indeed the case in the region close to the phase transition, while as the temperature decreases the deviation from the linear behavior becomes more visible. Figure 4(b) corresponds to the different normalization factor under the logarithm, T^2.

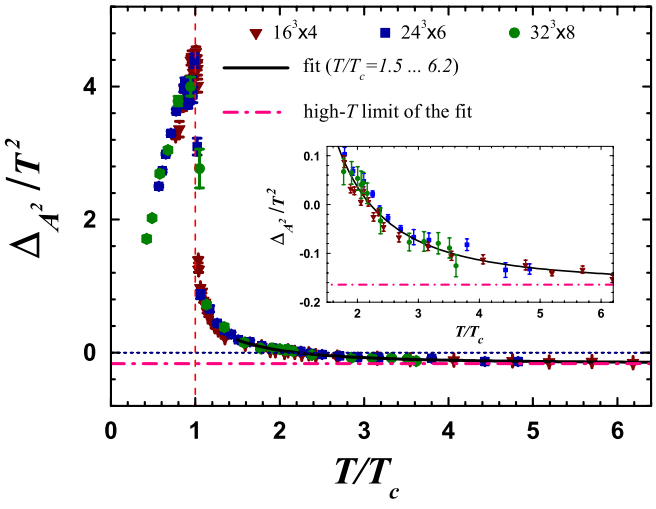

FIG. 3 (color online). The same as in Fig. 2 but for electric-magnetic asymmetry of the A^2 condensate (9) normalized by the temperature T^2. The inset zooms in on the high-temperature region of the fit. The peaked value at $T = T_c$, Eq. (40), and the asymptotic value at $T \to \infty$, Eq. (36), are indicated by vertical dotted and horizontal dash-dotted lines, respectively.

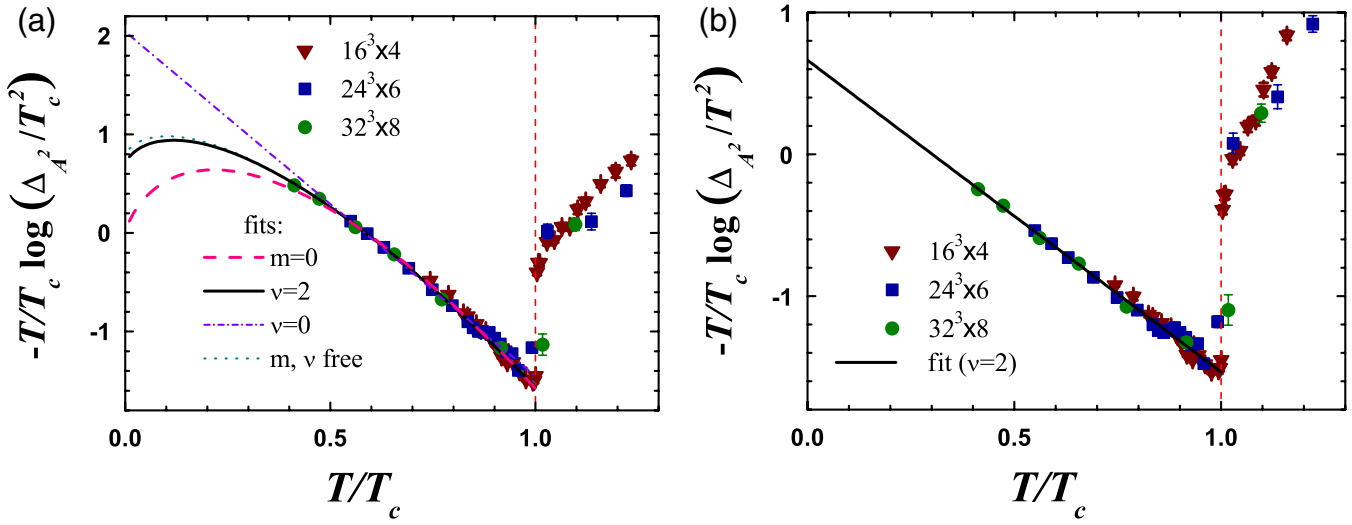

FIG. 4 (color online). The behavior of the electric-magnetic asymmetry in the low-temperature region. The lines represent the fits by the function (41), which are discussed in the text. Notice the different normalization of the expression under the logarithm: in (a) the normalization factor is $1/T_c^2$, while in (b) this factor is $1/T^2$.

First, we performed the fit using all three parameters C_Δ, ν, and m. The best fit parameters are presented in Table I, and the corresponding curve is shown in Fig. 4(a) by the dotted line. The fit was performed using all available values of the asymmetry in the low-temperature region, $T < T_c$. As one can see from the table, the exponent ν is quite close to 2, so that we have fixed $\nu = 2$ and performed another fit. The quality of both fits is characterized by almost the same value of χ^2/d.o.f., also presented in Table I. The fitting curve is shown in Fig. 4(a) by the solid line. Despite very good visual coincidence of the numerical data and the fitting curves, the high value of $\chi^2/\text{d.o.f.} \approx 6$ is due to the fact that the data corresponding to different lattice volumes are somewhat scattered with respect to each other in the region close to the phase transition. Since the transition is of second order, we attribute the high value of the χ^2/d.o.f. parameter to finite-volume effects.

The polynomial prefactor plays an important role. If we set $\nu = 0$, the fitting function reduces to a purely exponential behavior. In this case the quality of the fit deteriorates drastically. The best fitting curve is shown in Fig. 4(a) by the dotted curve. Similarly, if we set the mass to zero, $m = 0$, and fit the data using only C_Δ and ν as free parameters, the quality of the fit gets worse, represented by the dashed line in Fig. 4(a). Moreover, according to Table I, in this case the polynomial behavior would be—with a good accuracy—proportional to T^3 and not to the fourth power as one might have guessed from the example of the massive Abelian vector model (28). Thus, the most plausible fit is characterized by an exponential suppression with a quadratic prefactor:

$$\Delta_{A^2}^{\text{fit}} = C_\Delta T^2 \exp\{-m/T\}, \tag{42}$$

with

$$C_\Delta = 9.00(32), \qquad m = 201(8)\ \text{MeV}. \tag{43}$$

The best fit curve corresponding to the quadratic polynomial behavior (42) is also shown in Fig. 4(b). We show the specific function of the data, $-(T/T_c)\log\Delta_{A^2}/T^2$. This

TABLE I. The best fit parameters ν, m, and C_Δ, and the parameter χ^2/d.o.f. describing the electric-magnetic asymmetry by the fitting function (41) in the low-temperature region. The mentioned fitting curves are shown in Fig. 4. We also indicate the masses and the correlation lengths $\lambda = 1/m$ in physical units.

ν	m/T_c	C_Δ	χ^2/d.o.f.	m, MeV	$1/m$, fm
1.82(28)	0.80(19)	10.24(1.96)	6.6	244(58)	0.80(19)
2 [exact]	0.66(2)	9.00(32)	6.2	201(8)	0.98(4)
0 [exact]	2.04(3)	32.96(64)	14.	622(18)	0.32(1)
2.97(3)	0 [exact]	4.84(32)	9.6	0 [exact]	∞

function must be linear if the data obey the law (42), and this seems to fit the data. However, in order to figure out this fact with confidence, one needs to calculate the electric-magnetic asymmetry at lower temperatures (the lowest temperature available to us in our simulation was $T \approx 0.4T_c$).

There are two important remarks now in order.

(i) First, our data suggest that the behavior of the electric-magnetic asymmetry at low temperature is not proportional to the fourth power of temperature, as one could guess from the simple case of a massive photon (28). The behavior is rather exponential (42) with a polynomial prefactor. According to our discussion at the end of Sec. II B a purely polynomial behavior is guaranteed if the propagator in momentum space tends to a certain nonvanishing limit with vanishing momentum. The propagator in the Abelian Higgs model provides us with a clear example of such a behavior. According to our discussion, in the Abelian Higgs model the very reason for the purely polynomial behavior is the appearance of the "longitudinal" massless pole, $1/p^2$, in the integrand (B2) of the integral representation of the asymmetry (A11). The $1/p^2$ term enters this representation in the combination $D(p^2)/p^2$, and if the propagator $D(p^2)$ would vanish at low momenta as, for example, $D(p^2) \propto p^2$, then the polynomial behavior of the asymmetry would change to an exponential one.

Thus, the low-temperature behavior of the electric-magnetic asymmetry of the dimension-2 condensate in Yang-Mills theory may shed some light on the low-momentum behavior of the gluon propagator in momentum space.

Indeed, the integral representation of the A^2 condensate in the Abelian Higgs model (A11) is similar to the one in Yang-Mills theory (32), such that the same considerations may apply. The exponential suppression of the condensate at low temperatures may signal that the thermal gluon propagator at low momenta behaves softer than the tree-level propagator. We should admit that we do not have data at low enough temperatures to prove this fact firmly.

(ii) The second interesting observation is that the mass which governs the exponential falloff of the asymmetry at low temperatures is not the glueball mass, as naively expected (11). According to Eq. (43) this massive parameter is much smaller than the glueball mass (3), namely, of the order of $\Lambda_{\rm QCD}$, in other words, of the order of the critical temperature T_c, Eq. (43). Thus, the characteristic length that describes nonperturbative effects related to the A^2 condensates may be as large as 1 Fermi. This could explain the fact that the exploration of the low-momentum asymptotics of the gluon propagator requires relatively large lattices [31].

IV. DISCUSSION: CONFINEMENT AND ASYMMETRY OF THE CONDENSATE

It is extremely interesting to understand the physical reasons behind the observed behavior of the electric-magnetic asymmetry (Fig. 2). First of all, it is striking that in the confining region the A^2 condensate is *not* electric-magnetic symmetric. Instead, the asymmetry is positive and is growing with temperature up to its maximum which is realized just at the deconfinement phase transition. We know from the considered example of the Abelian Higgs model that a finite mass gap alone could not result in a positive value of the asymmetry. This suggests that the asymmetry of the dimension-2 condensate ought to be related to the purely confining properties of the system. This observation is in agreement with the original suggestion made in Refs. [2,3], as well as with numerical results of Ref. [32], in which a relation between the dimension-2 condensates and the confining string was discussed. Thus, one can conclude that color confinement (and its agents) may contribute to the unexpected behavior of asymmetry in the confinement phase.

It is generally accepted that the confinement of color can be explained by the dynamics of either monopolelike gluonic configurations (for a review see Ref. [11]) or by stringlike vortex configurations (a review can be found in Ref. [12]). In fact, these objects turn out to be interrelated physically [33–36] and geometrically [12]. Confinement of color in the low-temperature phase is caused by condensation of monopoles and by the spatial percolation of vortices.

Since the asymmetry of the A^2 condensate is presumably related to the color confinement, one should be able to trace the asymmetry back to the dynamics of the monopoles (and of the center vortices, but below we discuss the magnetic monopoles only). Moreover, the interactions of the electric charges and the magnetic monopoles are important to determine the state of the monopoles [29,30]. Therefore, it is very natural to suggest that the monopole dynamics leaves its footprints in the electric-magnetic asymmetry of the dimension-2 condensate.

We suggest that the increase of the electric-magnetic asymmetry in the confinement phase is related to a gradual decrease of the monopole condensate, as witnessed also by the decreasing string tension with $T \to T_c$ in $SU(2)$ gluodynamics. Once the condensate has disappeared at $T = T_c$, the asymmetry starts to become weaker. According to Refs. [28–30], in this region the monopoles form a monopole liquid. The heating of the liquid leads to its complete evaporation only at higher temperatures. According to Ref. [28] this should happen around $T \approx 2T_c$, which is pretty close to the point T_0 where the asymmetry vanishes (38). Thus, one can suggest that at $T = T_0$ the liquid predominantly turns into a monopole gas. The negative value of the electric-magnetic asymmetry of the A^2 con-

densate is characterized by the gaseous phase of the magnetic monopoles.

V. CONCLUSION

We have studied the electric-magnetic asymmetry of the A^2 condensate in the Landau gauge in three gauge theories at finite temperature in four space-time dimensions.

(i) In photodynamics—the free theory of a massless Abelian gauge field (12)—the asymmetry can be computed analytically. The asymmetry turns out to be negative for all temperatures. It is proportional to the temperature squared (19).

(ii) In the Abelian Higgs theory (20), for the London limit the analytical expression for the asymmetry is given by Eqs. (22)–(24). This theory corresponds basically to a free theory of a massive gauge field. The asymmetry—shown in Fig. 1—is also negative for all temperatures, and the high- and low-temperature limits can be computed, respectively, in Eqs. (27) and (28).

(iii) In the $SU(2)$ gauge theory we compute the electric-magnetic asymmetry using numerical simulations on the lattice (Fig. 2). The temperature dependence of the asymmetry turns out to be unexpected: at low temperatures the asymmetry is positive. It grows with increasing temperature, reaching a maximum around the critical temperature $T \approx T_c$. In the deconfinement phase the asymmetry drops rapidly with increasing temperature. At $T = T_0 = 2.21(5)T_c = 675(23)$ MeV the asymmetry vanishes, and it becomes negative at higher temperature.

In the spirit of Ref. [25], we suggest that the low-temperature asymptotics of the A^2 condensate is related to the low-momentum behavior of the gluon propagator. Our data at relatively low temperatures, $0.4T_c \lesssim T \lesssim T_c$, indicate that the asymmetry is suppressed exponentially (42), providing strong arguments in favor of the infrared suppression of the gluon propagator at low temperatures.

The mass, which governs the exponential low-temperature suppression of the asymmetry (42), is unexpectedly much smaller than the mass of the glueball. We found $m = 201(8)$ MeV, somewhat smaller than the deconfinement temperature T_c of the pure Yang-Mills theory. The corresponding correlation length, $\lambda = 1/m$, is of the order of 1 Fermi. As a by-product, this result suggests that relatively large (many Fermi in one direction) lattice volumes are needed to pin down the low-momentum asymptotics of the gluon propagator.

The electric-magnetic asymmetry is most probably related to the changing dynamics of the confining gluonic configurations, the magnetic monopoles. In fact, the monopole dynamics may be footprinted in the electric-magnetic asymmetry of the condensate because the electric degrees of freedom affect the properties of the magnetic monopoles [29,30] and vice versa. In more detail, the regions of (1) positive and growing, (2) positive and decreasing, and (3) negative asymmetry coincide with the regions in which the monopoles should, according to the classification of Ref. [28], (1) be condensed, (2) form a liquid state, and (3) form a predominantly gaseous state, respectively.

ACKNOWLEDGMENTS

M. N. Ch. was partly supported by Grant No. RFBR 06-02-04010-NNIO-a, No. RFBR 08-02-00661-a, joint German-Russian Grant No. DFG-RFBR 436 RUS, a grant for scientific schools (NSh-679.2008.2), by the Federal Program of the Russian Ministry of Industry, Science and Technology Grant No. 40.052.1.1.1112, and by the Russian Federal Agency for Nuclear Power. M. N. Ch. is also grateful for STINT Institutional Grant No. IG2004-2 025. E. M. I. is supported by DFG through the Forschergruppe FOR 465, and thanks his coauthors within the Adelaide-Berlin-Dubna-Moscow "Infrared QCD" Collaboration, in particular Vitaly Bornyakov, Valya Mitrjushkin, Michael Müller-Preussker, Lorenz von Smekal, and Andre Sternbeck, for cooperation and discussions on related questions.

APPENDIX A: THE ASYMMETRY IN PHOTODYNAMICS

The asymmetry of the condensate in the momentum representation is

$$\begin{aligned}\Delta_{A^2}(T) &= T\sum_n \int \frac{\mathrm{d}^3 p}{(2\pi)^3}\Big[\langle A_4(\mathbf{p},\omega_n)A_4(-\mathbf{p},-\omega_n)\rangle \\ &\quad - \frac{1}{3}\sum_{i=1}^{3}\langle A_i(\mathbf{p},\omega_n)A_i(-\mathbf{p},-\omega_n)\rangle\Big] \\ &\equiv T\sum_n \int \frac{\mathrm{d}^3 p}{(2\pi)^3}\Big[D_{44}(\mathbf{p},\omega_n) - \frac{1}{3}\sum_{i=1}^{3} D_{ii}(\mathbf{p},\omega_n)\Big] \\ &\equiv T\sum_n \int \frac{\mathrm{d}^3 p}{(2\pi)^3} G_{A^2}(\mathbf{p},\omega_n), \qquad \text{(A1)}\end{aligned}$$

where the momentum-dependent structure function of the asymmetry is

$$G_{A^2}(\mathbf{p},\omega_n) = D_{44}(\mathbf{p},\omega_n) - \frac{1}{3}\sum_{i=1}^{3} D_{ii}(\mathbf{p},\omega_n). \qquad \text{(A2)}$$

In order to proceed further, we use the following trick. It is well known [18,37] that sums over Matsubara frequencies (16) of the form (A2) can generally be converted into integrals,

$$T\sum_{n\in\mathbb{Z}} F(p_0 = i\omega_n) = \frac{1}{2\pi i}\int_{-i\infty+\epsilon}^{+i\infty+\epsilon} \mathrm{d}p_0\, \mathrm{Re}F(p_0) + \frac{1}{\pi i}\int_{-i\infty+\epsilon}^{+i\infty+\epsilon} \mathrm{d}p_0 f_T(p_0)\, \mathrm{Re}F(p_0), \qquad p_0 = ip_4, \tag{A3}$$

where $\epsilon \to +0$, the real part of the function F is defined as follows,

$$\mathrm{Re}\, F(p_0) \equiv \tfrac{1}{2}[F(p_0) + F(-p_0)], \tag{A4}$$

and the temperature-dependent function,

$$f_T(p_0) = \frac{1}{e^{p_0/T} - 1}, \tag{A5}$$

is the Bose-Einstein distribution of a bosonic particle with the energy $\omega = p_0$ at temperature T. Equation (A3) is valid for any analytical function $F(p_0)$, provided it does not possess poles at the imaginary p_0 axis.

It is easy to notice that the first term on the right-hand side of Eq. (A3) is temperature independent, and therefore it represents the zero-temperature part of the sum. Since the summation over Matsubara frequencies is usually supplemented with integration over the spatial momentum $\mathbf{p}$, the zero-temperature part can generally be divergent in the ultraviolet region. The second term is the temperature-dependent correction, which is usually finite because of the exponential suppression of the ultraviolet modes with $p_0 \gg 0$.

The sum (A2) over the asymmetry structure function G_{A^2},

$$\Delta_{A^2}(T) = \Delta_{A^2}(T=0) + \delta\Delta_{A^2}(T), \tag{A6}$$

with

$$\Delta_{A^2}(T=0) = \frac{1}{2i}\int\frac{\mathrm{d}^3p}{(2\pi)^3}\int_{-i\infty+\epsilon}^{i\infty+\epsilon}\frac{\mathrm{d}p_0}{2\pi} \times [C_A(\mathbf{p}, ip_0) + C_A(\mathbf{p}, -ip_0)] \tag{A7}$$

and

$$\delta\Delta_{A^2}(T) = \frac{1}{2i}\int\frac{\mathrm{d}^3p}{(2\pi)^3}\int_{-i\infty+\epsilon}^{i\infty+\epsilon}\frac{\mathrm{d}p_0}{2\pi}[C_A(\mathbf{p}, ip_0) + C_A(\mathbf{p}, -ip_0)]f_T(p_0), \tag{A8}$$

is expressed through the simple function

$$C_A(\mathbf{p}, p_4) = \frac{\mathbf{p}^2 - 3p_4^2}{3(p^2)^2}. \tag{A9}$$

One can explicitly check that

$$\Delta_{A^2}(T=0) = 0, \tag{A10}$$

as we have expected. This result is intuitively clear because at zero temperature the difference between spatial and temporal directions disappears, and therefore the space-time asymmetry of any quantity must be zero. Thus, only the temperature-dependent part of the A^2 condensates contributes to the asymmetry.

At nonzero temperature we represent the asymmetry as the sum of the residues

$$\Delta_{A^2}(T) = \delta\Delta_{A^2}(T) = \int\frac{\mathrm{d}^3p}{(2\pi)^3}\sum_{p_0>0} 2\,\mathrm{res}(\mathrm{Re}C_A(\mathbf{p}, ip_0)f(p_0)). \tag{A11}$$

The residue in the case of an nth order pole at $z = a$ is defined as

$$\mathrm{res}\, f(a) = \frac{1}{(n-1)!}\lim_{z\to a}\frac{\mathrm{d}^{n-1}}{\mathrm{d}z^{n-1}}[(z-a)^n f(z)], \tag{A12}$$

such that

$$\text{for } n = 1 \qquad \mathrm{res} f(z) = \lim_{z\to a}[(z-a)f(z)], \tag{A13}$$

$$\text{for } n = 2 \qquad \mathrm{res} f(z) = \lim_{z\to a}\frac{\mathrm{d}}{\mathrm{d}z}[(z-a)^2 f(z)]. \tag{A14}$$

The quantity in the integrand,

$$2(\mathrm{Re}C_A(\mathbf{p}, ip_0)f(p_0)) = \frac{2}{3}\frac{(\mathbf{p}^2 + 3p_0^2)f_T(p_0)}{(p_0 - |\mathbf{p}|)^2(p_0 + |\mathbf{p}|)^2}, \tag{A15}$$

has a double pole in the complex p_0 plane on the positive real axis at $p_0 = |\mathbf{p}|$. Using Eq. (A14) and then Eq. (A11), we get Eq. (19) for the case of the free massless photon.

APPENDIX B: THE ASYMMETRY IN THE ABELIAN HIGGS MODEL

In the Abelian Higgs model, instead of Eq. (A9) we get

$$C_A(\mathbf{p}, p_4) = \frac{\mathbf{p}^2 - 3p_4^2}{3(p^2)(p^2 + m^2)}, \tag{B1}$$

and therefore,

$$2(\mathrm{Re}C_A(\mathbf{p}, ip_0)f(p_0)) = \frac{2}{3}\frac{(\mathbf{p}^2 + 3p_0^2)f_T(p_0)}{[p_0^2 - \mathbf{p}^2][p_0^2 - (\mathbf{p}^2 + m^2)^2]}. \tag{B2}$$

Thus there are two single ($n = 1$) poles in the complex p_0 plane on the positive real axis at $p_0 = |\mathbf{p}|$ and $p_0 = \sqrt{\mathbf{p}^2 + m^2}$. Using Eq. (A13) we obtain

$$\mathrm{res}[2(\mathrm{Re}C_A(\mathbf{p}, ip_0)f(p_0))] = \frac{4}{3m^2}[\sqrt{\mathbf{p}^2+m^2}f_T(\sqrt{\mathbf{p}^2+m^2}) - |\mathbf{p}|f_T(|\mathbf{p}|)] - \frac{1}{3}\frac{f_T(\sqrt{\mathbf{p}^2+m^2})}{\sqrt{\mathbf{p}^2+m^2}}. \quad \text{(B3)}$$

Substituting this result in Eq. (A11) we get Eqs. (22)–(24).

[1] M. A. Shifman, A. I. Vainshtein, and V. I. Zakharov, Nucl. Phys. **B147**, 385 (1979).
[2] F. V. Gubarev, L. Stodolsky, and V. I. Zakharov, Phys. Rev. Lett. **86**, 2220 (2001).
[3] F. V. Gubarev and V. I. Zakharov, Phys. Lett. B **501**, 28 (2001).
[4] Ph. Boucaud, F. De Soto, J. P. Leroy, A. Le Yaouanc, J. Micheli, H. Moutarde, O. Pene, and J. Rodriguez-Quintero, Phys. Rev. D **74**, 034505 (2006).
[5] K. G. Chetyrkin, S. Narison, and V. I. Zakharov, Nucl. Phys. **B550**, 353 (1999); V. I. Zakharov, Nucl. Phys. B, Proc. Suppl. **164**, 240 (2007); **74**, 392 (1999).
[6] Ph. Boucaud, A. Le Yaouanc, J. P. Leroy, J. Micheli, O. Pene, and J. Rodriguez-Quintero, Phys. Rev. D **63**, 114003 (2001).
[7] C. Michael and M. Teper, Nucl. Phys. **B314**, 347 (1989).
[8] G. S. Bali, K. Schilling, A. Hulsebos, A. C. Irving, C. Michael, and P. W. Stephenson (UKQCD Collaboration), Phys. Lett. B **309**, 378 (1993).
[9] A. M. Polyakov, Nucl. Phys. **B120**, 429 (1977).
[10] T. Banks, R. Myerson, and J. B. Kogut, Nucl. Phys. **B129**, 493 (1977).
[11] M. N. Chernodub and M. I. Polikarpov, in *Confinement, Duality, and Nonperturbative Aspects of QCD*, edited by P. van Baal (Plenum Press, New York, 1998).
[12] J. Greensite, Prog. Part. Nucl. Phys. **51**, 1 (2003).
[13] S. Furui and H. Nakajima, Phys. Rev. D **76**, 054509 (2007).
[14] Ph. Boucaud, F. De Soto, A. Le Yaouanc, J. P. Leroy, J. Micheli, H. Moutarde, O. Pene, and J. Rodriguez-Quintero, Phys. Rev. D **67**, 074027 (2003).
[15] Ph. Boucaud, F. De Soto, J. P. Leroy, A. Le Yaouanc, J. Micheli, H. Moutarde, O. Pene, and J. Rodriguez-Quintero, Phys. Rev. D **74**, 034505 (2006).
[16] G. Boyd, J. Engels, F. Karsch, E. Laermann, C. Legeland, M. Lütgemeier, and B. Petersson, Phys. Rev. Lett. **75**, 4169 (1995).
[17] G. Boyd, J. Engels, F. Karsch, E. Laermann, C. Legeland, M. Lütgemeier, and B. Petersson, Nucl. Phys. **B469**, 419 (1996).
[18] J. I. Kapusta, *Finite-Temperature Field Theory* (Cambridge University Press, Cambridge, England, 1989).
[19] M. N. Chernodub, E.-M. Ilgenfritz, and A. Schiller, Phys. Rev. D **67**, 034502 (2003).
[20] A. Cucchieri, A. Maas, and T. Mendes, Phys. Rev. D **75**, 076003 (2007).
[21] A. Maas, Mod. Phys. Lett. A **20**, 1797 (2005).
[22] B. Grüter, R. Alkofer, A. Maas, and J. Wambach, Eur. Phys. J. C **42**, 109 (2005).
[23] A. Maas, J. Wambach, and R. Alkofer, Eur. Phys. J. C **42**, 93 (2005).
[24] A. Maas, J. Wambach, B. Grüter, and R. Alkofer, Eur. Phys. J. C **37**, 335 (2004).
[25] M. N. Chernodub and V. I. Zakharov, Phys. Rev. Lett. **100**, 222001 (2008).
[26] G. S. Bali, V. G. Bornyakov, M. Müller-Preussker, and K. Schilling, Phys. Rev. D **54**, 2863 (1996).
[27] J. Fingberg, U. M. Heller, and F. Karsch, Nucl. Phys. **B392**, 493 (1993); M. J. Teper, arXiv:hep-th/9812187.
[28] M. N. Chernodub and V. I. Zakharov, Phys. Rev. Lett. **98**, 082002 (2007).
[29] J. Liao and E. Shuryak, Phys. Rev. C **75**, 054907 (2007).
[30] J. Liao and E. Shuryak, arXiv:0804.0255.
[31] A. Cucchieri and T. Mendes, Proc. Sci., LAT2007 (2007) 297 [arXiv:0710.0412]; I. L. Bogolubsky, E.-M. Ilgenfritz, M. Müller-Preussker, and A. Sternbeck, Proc. Sci., LAT2007 (2007) 290 [arXiv:0710.1968].
[32] M. N. Chernodub, K. Ishiguro, Y. Mori, Y. Nakamura, M. I. Polikarpov, T. Sekido, T. Suzuki, and V. I. Zakharov, Phys. Rev. D **72**, 074505 (2005).
[33] J. Ambjorn, J. Giedt, and J. Greensite, J. High Energy Phys. 02 (2000) 033.
[34] V. I. Zakharov, AIP Conf. Proc. **756**, 182 (2005).
[35] P. Yu. Boyko, V. G. Bornyakov, E.-M. Ilgenfritz, A. V. Kovalenko, B. V. Martemyanov, M. Müller-Preussker, M. I. Polikarpov, and A. I. Veselov, Nucl. Phys. **B756**, 71 (2006).
[36] V. G. Bornyakov, E.-M. Ilgenfritz, M. Müller-Preussker, B. V. Martemyanov, S. M. Morozov, and A. I. Veselov, Phys. Rev. D **77**, 074507 (2008).
[37] M. B. Kislinger and P. D. Morley, Phys. Rev. D **13**, 2771 (1976).